Applied Physics Letters

RESEARCH ARTICLE | JUNE 12 2023

Room temperature colossal superparamagnetic order in aminoferrocene–graphene molecular magnets FREE

Yohannes W. Getahun ; Felicia S. Manciu ; Mark R. Pederson ; Ahmed A. El-Gendy

Appl. Phys. Lett. 122, 241903 (2023)
https://doi.org/10.1063/5.0153212
CHORUS

AIP Publishing

Applied Physics Letters ARTICLE pubs.aip.org/aip/apl

Room temperature colossal superparamagnetic order in aminoferrocene–graphene molecular magnets

Cite as: Appl. Phys. Lett. **122**, 241903 (2023); doi: 10.1063/5.0153212
Submitted: 5 April 2023 · Accepted: 29 May 2023 ·
Published Online: 12 June 2023

View Online Export Citation CrossMark

Yohannes W. Getahun,[1,2] Felicia S. Manciu,[1] Mark R. Pederson,[1] and Ahmed A. El-Gendy[1,a)]

AFFILIATIONS

[1]Department of Physics, University of Texas at El Paso, El Paso, Texas 79968, USA
[2]Environmental Science and Engineering, Material Science & Engineering, University of Texas at El Paso, El Paso, Texas 79968, USA

[a)]Author to whom correspondence should be addressed: aelgendy@utep.edu

ABSTRACT

Intensive studies are published for graphene-based molecular magnets due to their remarkable electric, thermal, and mechanical properties. However, to date, most of all produced molecular magnets are ligand based and subject to challenges regarding the stability of the ligand(s). The lack of long-range coupling limits high operating temperature and leads to a short-range magnetic order. Herein, we introduce an aminoferrocene-based graphene system with room temperature superparamagnetic behavior in the long-range magnetic order that exhibits colossal magnetocrystalline anisotropy of 8×10^5 and 3×10^7 J/m^3 in aminoferrocene and graphene-based aminoferrocene, respectively. These values are comparable to and even two orders of magnitude larger than pure iron metal. Aminoferrocene $[C_{10}H_{11}FeN]^+$ is synthesized by an electrophilic substitution reaction. It was then reacted with graphene oxide that was prepared by the modified Hammers method. The phase structure and functionalization of surface groups were characterized and confirmed by XRD, FT-IR, and Raman spectroscopy. To model the behavior of the aminoferrocene between two sheets of hydroxylated graphene, we have used density functional theory by placing the aminoferrocene molecule between two highly ordered hydroxylated sheets and allowing the structure to relax. The strong bowing of the isolated graphene sheets suggests that the charge transfer and resulting magnetization could be strongly influenced by pressure effects. In contrast to strategies based on ligands surface attachment, our present work that uses interlayer intercalated aminoferrocene opens routes for future molecular magnets as well as the design of qubit arrays and quantum systems.

Since the discovery of molecular magnets (MMs),[1,2] there has been growing interest in developing molecular materials that can exhibit cooperative magnetic interactions at room temperature. Molecular magnets (MMs) are classes of magnetic materials, in which molecular moieties bearing unpaired spin density interact electronically and magnetically.[1,3] Because of their quantum size effects, lightweight, mechanical flexibility, tunable color or transparency, low-temperature processing, solubility, and compatibility with polymers and other classes of molecular materials, MMs have great advantages and unique properties compared to conventional magnets in high-density data storage. Furthermore, the use of MMs in spintronic and qubits for quantum computing has the potential to become a disruptive technology, since organic materials can enhance preservation of electron spin orientation lifetime relative to inorganic conductors due to their inherently weak spin–orbit coupling. However, producing room temperature molecular magnets was and still is a challenge. There is only the work done by Manriquez *et al.*,[4] where it was shown that the reaction ring of bis(benzene)vanadium with tetracyanoethylene (TCNE) affords an insoluble amorphous black solid that exhibits ferromagnetism at room temperature. The origin of the magnetic behavior was based on three-dimensional antiferromagnetic exchange of the donor and acceptor spins resulting in ferromagnetic behavior. Then, this work has been continued to include other 3d metals, such as Mn.[5] Since then, scientists have been focusing on the development of molecular magnets that operate near room temperature with the goal of enabling spintronic applications. Recently, a MM system has been discovered by Guo *et al.*[6] that contains dysprosium metallocene with magnetic hysteresis observed up to 70 K. Such behavior originates from spin-phonon coupling regimes. Since the discovery of graphitic carbon in 1991 by Ijima,[7] there has been working on developing magnetic graphene or graphene based molecular magnets that might show a room temperature ferromagnetic behavior.[8–10] In addition, ligand

based molecular magnets suffer from tunneling at zero field, a major cause for their inefficiency for information storage.[11–18] Even though graphene sheets lack magnetic property, structural change due to oxidation to graphene oxide and structural defects might introduce ferromagnetism.[12,13] In both graphene oxide and reduced graphene oxide, Diamantopoulou *et al.*[12] and Sarkar *et al.*[13] reported weak magnetism at room temperature. Epoxide functional group composites are responsible for magnetic susceptibility of graphene oxide,[14] creating unpaired spins on the carbon radicals.[15,16] In a recent study, attachment of electron withdrawing substituted ligands to the graphene enhanced the charge transfer revealing magnetic and electronic properties.[19]

In this study, we aimed to solve two major technical impediments for use and delivery of graphene-based molecular magnets (G-MMs). The first is the challenge to synthesize molecular magnets that can operate at room temperature. The second is to increase magnetic order stability by attempting to locate the ligand inside the layers and rely upon slight metallic behavior to increase the onsite magnetic anisotropy and strongly couple neighboring magnetic intercalants. For this reason, we select aminoferrocene for its efficacy to participate in electron transfer[20–25] to be intercalated within the graphene oxide layers. Herein, two graphene oxide-based aminoferrocene molecular magnets are used GO-MM1 and GO-MM2. They are both molecular magnets with the same type, amount, and composition of reactants but different synthesis procedures. GO-MM1 is synthesized in a two-step reaction. The first step was synthesis of charged aminoferrocene as in the following procedure.

To obtain the required compound, i.e., charged aminoferrocene, ferrocene is reacted with conc. H_2SO_4 in conc. HNO_3 [both acids generate an electrophile called nigronium ion known as nigronium ion (NO^{2+})] that breaks the delocalization in the cyclopentadiene ring and nitro-ferrocene. Then, by adding Sn in conc. HCl, heat will be reduced from the nitro group to amino group. Finally, sulfate byproduct will neutralize the positive charge on nitrogen by proton abstraction. The resultant sulfuric acid will give a proton and abstract a hydrogen ion from the iron (Fig. S1). GO-MM2 is prepared in one pot synthesis, that is, all reactants including ferrocene were added simultaneously and resulted in a non-magnetic system. We believe that the charged aminoferrocene failed to form; hence, the source of spin for the entire molecular magnet is missing.

The crystal structure was characterized using XRD as shown in Fig. 1. A sharp peak at a range of 10° is a good signifier of graphene oxide formation.[33] Our calculation of the interlayer spacing using the Bragg law [order of reflection (n) × wavelength (λ) = 2 × interplanar spacing (d) × $\sin\theta$, where λ—wavelength of incident x ray, theta(θ) = peak position in radians] also indicated that GO layers have wider spacing (d_{001} = 1.0365 nm) than the repeatedly reported d-spacing, which is less than 1 nm.[33–35] This spacing will be filled with aminoferrocene sandwiched between the layers.[34] In addition to the weak van der Waals interaction existed between the double conjugation of the graphene oxide and the diene in ferrocene,[36] the hydrogen bonding within the amino-group of ferrocene and oxygen of the GO-layer might have contributed to the stabilization of the interaction. The strongest interaction is expected to be coulombic due to charge transfer between the aminoferrocene and the bilayer. In addition, as seen in Fig. 1, the XRD peaks confirm the presence of the aminoferrocene and the Go-aminoferrocene molecular magnets and no presence for any related iron oxide phase structure.

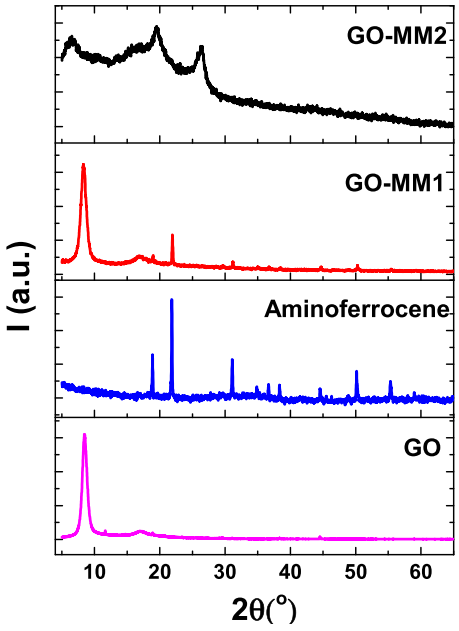

FIG. 1. XRD spectra of GO-MM2, GO-MM1, aminoferrocene $[C_{10}H_{11}FeN]^+$, and graphene oxide.

To verify the presence of the functional groups, FT-IR studies were performed under vacuum in the transmission mode. For easier comparison and vibrational line assignments, in addition to the IR spectra of GO-MM1 and GO-MM2 samples, the aminoferrocene spectrum is also presented in Fig. 2. The spectrum shows dominant vibrational lines at 520 (ring–Fe–ring stretching), 968 (CH bending), 1120 (anti-symmetric cyclopentadienyl ring breathing mode), 1384 (CC stretching), 1530 (CC stretching), 1658 (CO, CC, and the amino

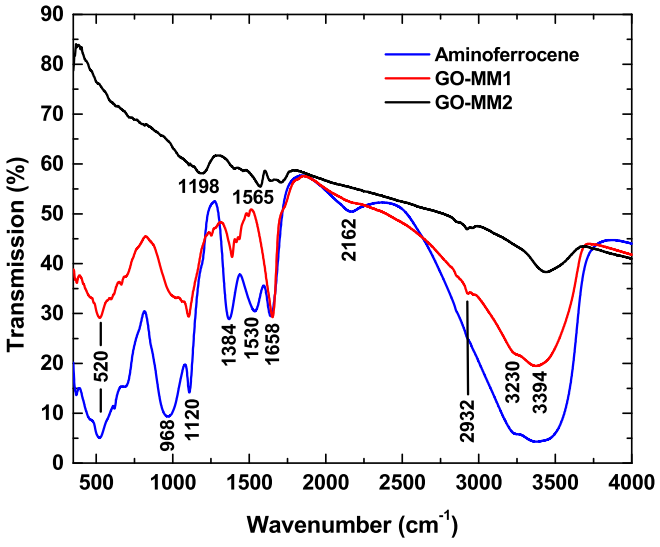

FIG. 2. FT-IR spectra of aminoferrocene $[C_{10}H_{11}FeN]^+$(blue line), GO-MM1(red line), and GO-MM2 (black line).

group stretching), 2162 (CO and CC stretching), 3230 (CH and OH stretching), and 3394 cm^{-1} (OH stretching).[41] All these aminoferrocene vibrational lines exhibit shifts of ~35 cm^{-1} on average from the vibrational frequencies' characteristic to ferrocene.[41] A quick comparison between the IR spectra of GO-MM1 and GO-MM2 samples with the spectrum of aminoferrocene reveals a much stronger presence of aminoferrocene in the GO-MM1 sample, presence almost absent in the case of the GO-MM2 sample. This remark is based on the similarity of vibrational lines observed in both the GO-MM1 and the aminoferrocene spectra. However, a closer look at these two spectra demonstrates that there are some vibrational differences, such as the decreases in the intensities of the 968 and 1384 cm^{-1} bands and the disappearances of the 1530 and 2162 cm^{-1} vibrations in the GO-MM1 spectrum. While these observations suggest a potential interaction between GO and aminoferrocene, it also masks the visualization of the characteristic GO vibrational modes, which can be depicted only by the weak vibrations at 2932 (sp^2 CH stretching) and 3230 cm^{-1} (OH stretching).[20,36] GO contains epoxide and hydroxyl functional on its basal plane, as well as carboxyl moieties at its edges, these two IR vibrations could be also associated with produced defects on the graphene network.[15,33] The IR spectrum of GO-MM2 shows the absence of the aminoferrocene absorptions at 520, 968, 1384, and 2162 cm^{-1}, upshifting of the aminoferrocene lines at 1120 and 1530 cm^{-1} to 1198 and 1565 cm^{-1}, respectively. It also shows a slightly more visible presence of GO, with characteristics vibrations at 1630 (CC stretching) and 1730 cm^{-1} (C=O stretching), besides those already observed in the GO-MM1 spectrum at 2932 and 3230 cm^{-1}. The absence of 2162 cm^{-1} feature in both spectra of GO-MM samples, vibrational lines that could also be assigned to −N=C=O groups, implies a potential intercalation/absorption of aminoferrocene between GO layers or at its edges. It also could imply a complete reaction of the organic material with the hydroxyl groups of GO.

To verify the presence of the aminoferrocene and graphene in the samples, Raman spectra of the GO-MM1 and GO-MM2 samples together with the aminoferrocene spectrum have been measured and are presented in Fig. 3. It is conventional to investigate the quality of a carbon-based sample by employing the intensity and broadness of the characteristic GO Raman features, the D and G bands, with the D mode known to correspond to the disordered carbon line and the related symmetry lowering or finite-size effects in GO, and the G mode related to the graphitic sample properties.[37–40] The observed D and G peaks in Fig. 5 at 1336 and at 1598 cm^{-1}, respectively, as well as the 2D bands at 2678 and 2935 cm^{-1} are in good agreement with their reported literature values.[37–40] A comparison between the Raman spectra of the GO-MM1 and GO-MM2 samples reveals an enhancement of the G peak in the spectrum of the former sample. This increase in the ratio of the intensity of the D peak to that of the G peak, ID/IG, from a 1.1 to 1.4 value for the GO-MM1 and GO-MM2 samples, respectively, is an indicative of a recovery of sp^2 domains in the GO and a reduction of its surface. This observation corroborates with the information obtained from other techniques used to analyze the samples, such as XRD and FT-IR. A slight increase is also observed in the intensities of 2D bands in the case of GO-MM2 sample, being attributed to the restoration of C–C interatomic distances and angles characteristic to GO. Also, the absence of the intense ferrocene vibrational lines at 307 (ring–Fe–ring stretching), 391 (ring–Fe–ring stretching), 1108 (symmetric ring breathing mode), and 3100 cm^{-1}

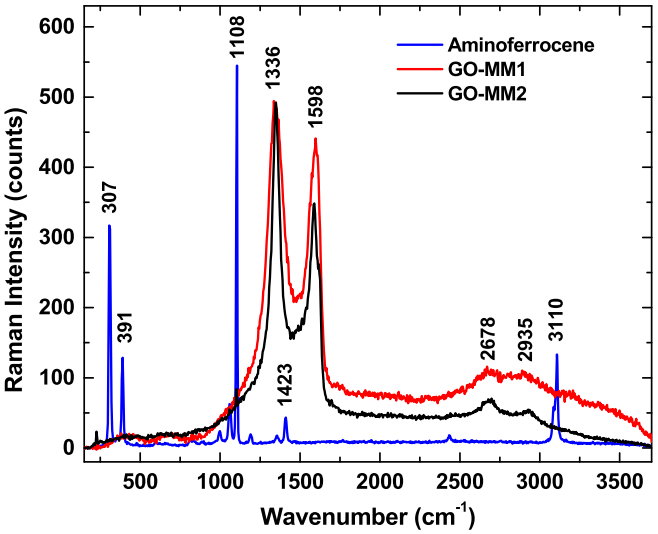

FIG. 3. Raman spectra of aminoferrocene (blue line), GO-MM1 (red line), and GO-MM2 (black line).

(symmetric CH stretching)[41] in the spectra of the two GO-MM samples again indicates a potential interaction between the organic material with the GO, in agreement with our FT-IR analysis. Moreover, the Raman spectra of GO in GO-MM1 are a single layer (2678 cm^{-1}), whereas in GO-MM2, it is three-layer (2701 cm^{-1}).[42]

To determine the magnetic range order of the prepared systems, magnetic measurements were carried out by using the vibrating sample magnetometer (VSM) in the magnetic field range of -3 to 3 T and the temperature range from 50 to 400 K. The measurements include hysteresis loop at room temperature (300 K), 50 K, and 350 K and the magnetization dependence on temperature at a constant magnetic field of 200 Oe.

Aminoferrocene and GO-MM1 displayed closed hysteresis loops at room temperature with coercivity (H_C) close to zero of 0.34 and 12.82 Oe [Fig. 4(a) inset], respectively, revealing superparamagnetic behavior with magnetization (Ms) of 3.06 and 2.762 emu/g and GO-MM2 showed paramagnetic behavior [Fig. 4(a)]. The M × T data were recorded by the ZFC/FC measurements at 200 Oe, which show the long-range magnetic order up to 400 K and confirm the superparamagnetic behavior of the aminoferrocene and GO-MM1 samples with blocking temperature (T_B) of 75 and 95 K, respectively [Fig. 4(b)]. There are two steps in the red curves, which are due to the presence of graphene to confirm the presence of two magnetic phases in the GO-MM1 sample. The GO-MM2 shows zero magnetization with no magnetic range order. The M × H data at 50 and 350 K show superparamagnetic behavior, which confirm the long-range magnetic order of the aminoferrocene and GO-MM1 samples, and show paramagnetic behavior for the GO-MM2 sample [Figs. 4(c) and 4(d)]. Since the samples have superparamagnetic behavior, the magnetocrystalline anisotropy was determined using Neel–Brown equation.[43] The aminoferrocene and GO-MM1 samples show colossal magnetocrystalline anisotropy with 3×10^7 and 8×10^5 J/m^3, respectively. These values are comparable with pure iron metal for graphene-based aminoferrocene (GO-MM1) and two order of magnitude larger than pure iron and one order of

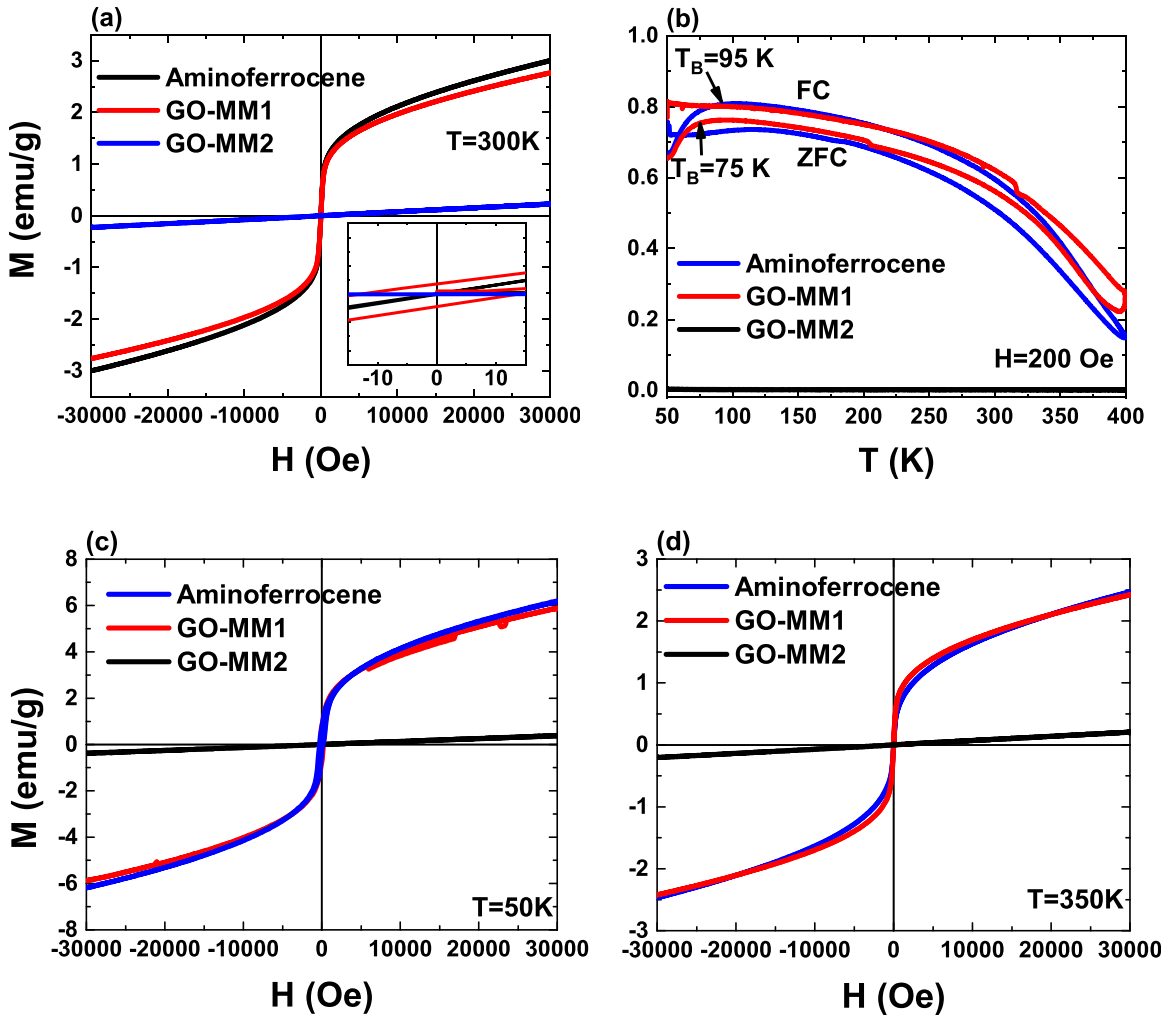

FIG. 4. Hysteresis loop at 300 K (a), magnetization at zero-field-cooled (ZFC) and field-cooled (FC) at 200 Oe (b), and magnetization dependence of external magnetic field at 50 (c) and 350 K (d).

magnitude larger than CoFeC permanent magnet for aminoferrocene molecular magnets.[43,44] Since the charged aminoferrocene persists, the reason for magnetization is due to electron withdrawing and deactivating effect of the charged nitrogen that is more electronegative than neighboring atoms. This decreases the π—electron density, while increasing the σ—electron density, in ortho and para positions of the ring creating a paramagnetic coupling, and de-shielding was resulted between the occupied σ with the unoccupied π orbitals and the unoccupied π^* orbitals with the occupied σ orbitals.[45] The interaction between π-orbitals in the sp2-bonded carbon atoms of graphene oxide sheets[21,46,47] and aminoferrocene contributes to the magnetization of the graphene oxide assembly.[39] Furthermore, the magnetic de-shielding effect of charged amino group facilitates magnetic field stream between each of these two agents.[45] This interaction is further stabilized by hydrogen bond, stronger intermolecular interaction between the amino group, and the nearby oxygen layers of the hydroxide or epoxide groups if aminoferrocene locates at the C-axis (center) of the layer. If the aminoferrocene is at the edges, its interaction with OH of the carboxyl group will lead to different arguments, which also make electron transfer very difficult. In a separate experiment, we changed the synthesis into a one-step mechanism where all the ingredients are added at once, including the separate procedure for preparation of aminoferrocene. The product (GO-MM2) was non-magnetic at room temperature. Clearly, aminoferrocene should not be formed in this assembly because the nitration and reduction process should be done separately.

In order to understand the reason for the observed magnetic properties in the aminoferrocene and GO-MM1, we have done theoretical studies using density of function theory (DFT) to verify the energy stability for the aminoferrocene to persist in between the layers. This interaction is exhibited constant energy with that bridge positions. In this case, aminoferrocene is situated perpendicular to both the layers. It was also found out that this bind energy is comparable to that of calculated benzene adsorption on graphene.[36] Within the generalized-gradient approximation for the aminoferrocene,

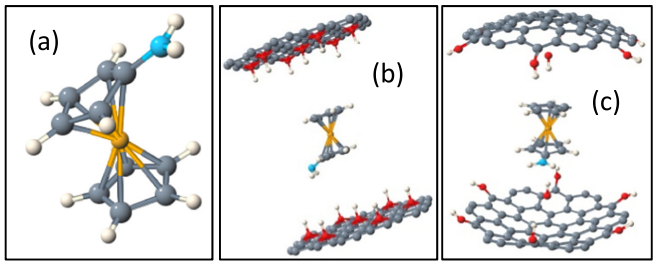

FIG. 5. Gas-phase structure of aminoferrocene (a) and the unrelaxed (b) and relaxed (c) $[C_{54}(OH)_7]_2$@ $Fe[C_5H_5C_5H_4NH_2]$ system.

$C_5H_5FeC_4H_4NH_2$, the neutral molecule resides in a singlet state and as expected from its iso-electronic counterpart, ferrocene, it has a large HOMO/LUMO gap. However, if two electrons are removed, the dication converts to an S = 1 state with two unpaired d-electrons on the Fe^{+2} center. The system has a HOMO/LUMO gap of 0.62 eV in the gas phase, the dication has a magnetic anisotropy of 9.1 K, and it is primarily easy axis albeit with an appreciable transverse anisotropy due to the presence of the amine group. For the gas-phase dication, there is significant departure from parallel pentacene planes in the gas phase as shown in Fig. 5. To model the behavior of the aminoferrocene between two sheets of hydroxylated graphene, we placed the molecule between two highly ordered hydroxylated sheets and allowed the structure to relax. For the overall neutral structures, several structural effects are observed. First, the OH radicals migrate away from the interior of the parallel sheets and bind to dangling bonds on the graphene sheets those have been identified in previous work.[26–32] Second, there is a significant internal pressure induced by the presence of the aminoferrocene Island, which leads to the isolated graphene sheets taking on a spherical shape. Third, the OH radicals at the center of the parallel sheets steal some electrons from the aminoferrocene, which causes a moment to form on the aminoferrocene. Based on numerical analyses of charge near the Fe ion, it appears that full charge transfer of two electrons to the two OH radicals does not appear (Table S1). The distortion of the aminoferrocene, found in the gas-phase dication, also does not occur as dramatically, which is in accord with an incompletely ionized island. The strong bowing of the isolated graphene sheets suggests that the charge transfer and resulting magnetization could be strongly influenced by pressure effects.

We have calculated the vibrational spectra of the aminoferrocene in the neutral and +2 charge state (S3). There is a qualitative difference in the Raman spectra at 1500 1/cm, which should be a very clear indicator of the S = 1 aminoferrocene. From the charge transfer analysis (Table S2), the structural effects suggest that, at least within Perdew–Burke–Ernzerhof generalized gradient approximation (PBE-GGA), the capacity for electron withdrawing of the OH radicals from the aminoferrocene is not, by itself, strong enough to create a dication with strong anisotropy between the two-graphene sheets. For the OH case, the calculated moment in charge suggests that a half of an electron is shared with the two OH radicals. These findings confirm the experimental observation of the magnetic order in both the aminoferrocene and GO-MM1 systems. We note that vdW interactions are not responsible for the attractions between infinite sheets of graphite or for attractions between the graphene flakes studied here. In our case, electrostatic interactions, properly included within DFT formulations, hold the flakes together.

From the above-mentioned findings on the magnetic order with superparamagnetic behavior of the aminoferrocene and GO-MM1 samples, the effect of the temperature on the direction and the fluctuation time of the magnetic moment of the angular crystalline radius of the prepared molecular magnets could be condensed into a single simple 3D figure (Fig. 6). Figures 6(a) and 6(b) represent the effect of temperature on the rotation of the magnetic moment for the aminoferrocene and GO-MM1, respectively. The color indicates the change in the temperature range starting from the lower temperatures (blue regions) up to the very high temperatures (black regions). The effect of the thermal energy on change of the magnetic moment direction has been implied from 0° to 12° for the aminoferrocene molecular magnets [Fig. 6(a)] and from 0° to 80° [Fig. 6(b)] resulting in a magnetic moment rotation image of the particle around its easy axis. Such small effect of the thermal energy on the angle confirms the presence of the long magnetic range order obtained from the experimental measurements for the aminoferrocene, which is longer and more stable than the GO-MM1 molecular magnet, which verify the observed colossal magnetocrystalline anisotropy energy. These findings open routes of room temperature long-range order molecular magnets and their potential for quantum computing and data storage applications.

Unlike graphene oxide, aminoferrocene in its ionic form was synthesized to appositely locate it between graphene oxide layers. The as-synthesized aminoferrocene molecular magnet shows unexpected colossal magnetocrystalline anisotropy with two order of magnitude larger than pure iron (Fe) and an order of magnitude larger than $CoFe_2C$ magnet. Such colossal anisotropy leads to thermal stable long-range superparamagnetic order. The magnetic order originates from

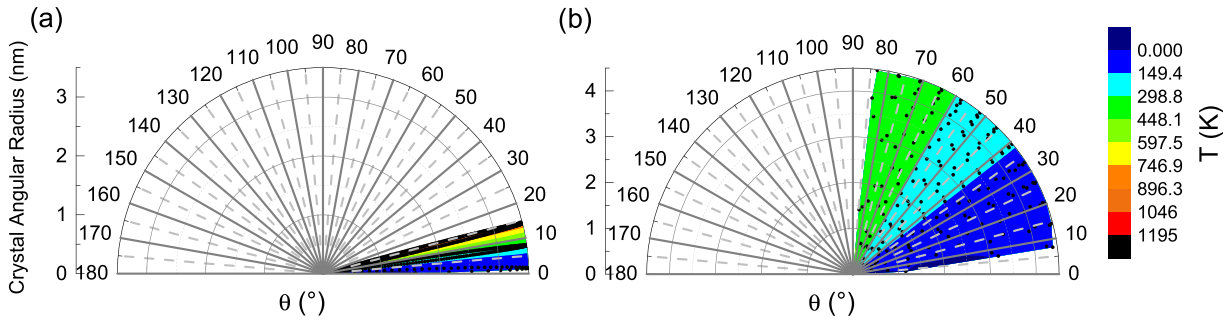

FIG. 6. Magnetocrystalline moment rotation under applied thermal energy revealing long-range order of (a) aminoferrocene and (b) GO-MM1 molecular magnets.

electron withdrawing capacity of the electron deficient nitrogen. Within the layers, this effect will transcend to the layers to enhance magnetization in addition to interaction of double bond electrons between each ring. The DFT data predict a metallization of the dihydroxylated aminoferrocene system with a total Fe to OH charge transfer of 0.63 electrons. The DFT calculations confirm the experimental observation of the magnetic order in aminoferrocene and GO-MM1 systems. This outstanding observation opens routes for room temperature molecular magnets, which will have a great potential in spintronic and quantum computing devices.

See the supplementary material that includes details of the materials and methods used to produce the synthesized MMs.

The authors acknowledge, with pleasure, support from the National Science Foundation (NSF) with Grant No. 2009358 and DOE-BES M2QM Energy Frontier Center (No. DE-SC001930). M.R.P. acknowledges the support by the Dr. C. Sharp Cook Endowed Chair. A.A.E. acknowledges the startup and rising stars funds by UTEP and UT-system, respectively.

AUTHOR DECLARATIONS

Conflict of Interest

The authors have no conflicts to disclose.

Author Contributions

Yohannes Getahun: Data curation (equal); Formal analysis (supporting); Investigation (equal); Methodology (equal); Writing – original draft (equal). **Felicia Speranta Manciu:** Formal analysis (supporting); Investigation (supporting); Validation (supporting); Writing – original draft (supporting). **Mark R. Pederson:** Data curation (equal); Methodology (supporting); Resources (supporting); Software (lead); Validation (equal); Writing – original draft (supporting); Writing – review & editing (supporting). **Ahmed A. El-Gendy:** Conceptualization (lead); Data curation (lead); Formal analysis (lead); Funding acquisition (lead); Investigation (lead); Methodology (lead); Project administration (lead); Resources (lead); Supervision (lead); Validation (equal); Visualization (lead); Writing – original draft (lead); Writing – review & editing (lead).

DATA AVAILABILITY

The data that support the findings of this study are available within the article and its supplementary material.

REFERENCES

[1]E. Coronado, "Molecular magnetism: From chemical design to spin control in molecules, materials and devices," Nat. Rev. Mater. **5**, 87–104 (2019).
[2]D. Luneau, "Molecular magnets," Curr. Opin. Solid State Mater. Sci. **5**, 123–129 (2001).
[3]O. Kahn, "Dinuclear complexes with predictable magnetic properties," Angew. Chem. **24**, 834–850 (1985).
[4]J. M. Manriquez, G. T. Yee, R. S. McLean, A. J. Epstein, and J. S. Miller, "A room-temperature molecular/organic-based magnet," Science **252**, 1415–1417 (1991).
[5]C. S. Olson, S. Gangopadhyay, K. Hoang, F. Alema, S. Kilina, and K. Pokhodnya, "Magnetic exchange in Mn II [TCNE] (TCNE = tetracyanoethylene) molecule-based magnets with two- and three-dimensional magnetic networks," J. Phys. Chem. C **119**(44), 25036–25046 (2015).
[6]F.-S. Guo, M. He, G.-Z. Huang, S. R. Giblin, D. Billington, F. W. Heinemann, M.-L. Tong, A. Mansikkamäki, and R. A. Layfield, "Discovery of a dysprosium metallocene single-molecule magnet with two high-temperature Orbach processes," Inorg. Chem. **61**, 6017–6025 (2022).
[7]S. Iijima, "Helical microtubules of graphitic carbon," Nature **354**, 56–58 (1991).
[8]S. J. Blundell and F. L. Pratt, "Organic and molecular magnets," J. Phys.: Condens. Matter **16**, R771–R828 (2004).
[9]J. Hong, E. Bekyarova, W. A. de Heer, R. C. Haddon, and S. Khizroev, "Chemically engineered graphene-based 2D organic molecular magnet," ACS Nano **7**, 10011–10022 (2013).
[10]M. Sakurai, P. Koley, and M. Aono, "Tunable magnetism of organometallic nanoclusters by graphene oxide on-surface chemistry," Sci. Rep. **9**, 14509 (2019).
[11]W. Wernsdorfer, N. Aliaga-Alcalde, D. N. Hendrickson, and G. Christou, "Exchange-biased quantum tunneling in a supramolecular dimer of single-molecule magnets," Nature **416**, 406–409 (2002).
[12]A. Diamantopoulou, S. Glenis, G. Zolnierkiwicz, N. Guskos, and V. Likodimos, "Magnetism in pristine and chemically reduced graphene oxide," J. Appl. Phys. **121**, 043906 (2017).
[13]S. K. Sarkar, K. K. Raul, S. S. Pradhan, S. Basu, and A. Nayak, "Magnetic properties of graphite oxide and reduced graphene oxide," Physica E **64**, 78–82 (2014).
[14]D. Galpaya, M. Wang, G. George, N. Motta, E. Waclawik, and C. Yan, "Preparation of graphene oxide/epoxy nanocomposites with significantly improved mechanical properties," J. Appl. Phys. **116**, 053518 (2014).
[15]D. Lee, J. Seo, X. Zhu, J. M. Cole, and H. Su, "Magnetism in graphene oxide induced by epoxy groups," Appl. Phys. Lett. **106**, 172402 (2015).
[16]M. Wang and C. M. Li, "Magnetism in graphene oxide," New J. Phys. **12**, 083040 (2010).
[17]Y. Liu, N. Tang, X. Wan, Q. Feng, M. Li, Q. Xu, F. Liu, and Y. Du, "Realization of ferromagnetic graphene oxide with high magnetization by doping graphene oxide with nitrogen," Sci. Rep. **3**, 2566 (2013).
[18]Y. Liu, Q. Feng, N. Tang, X. Wan, F. Liu, L. Lv, and Y. Du, "Increased magnetization of reduced graphene oxide by nitrogen-doping," Carbon **60**, 549–551 (2013).
[19]X. Zhu, A. Hale, G. Christou, and A. F. Hebard, "Electronegative ligands enhance charge transfer to Mn_{12} single-molecule magnets deposited on graphene," J. Appl. Phys. **127**, 064303 (2020).
[20]L. Guan, Z. Shi, M. Li, and Z. Gu, "Ferrocene-filled single-walled carbon nanotubes," Carbon **43**, 2780–2785 (2005).
[21]M. Lopes, A. Candini, M. Urdampilleta, A. Reserbat-Plantey, V. Bellini, S. Klyatskaya, L. Marty, M. Ruben, M. Affronte, W. Wernsdorfer, and N. Bendiab, "Surface-enhanced Raman signal for terbium single-molecule magnets grafted on graphene," ACS Nano **4**, 7531–7537 (2010).
[22]N. I. Zaaba, K. L. Foo, U. Hashim, S. J. Tan, W.-W. Liu, and C. H. Voon, "Synthesis of graphene oxide using modified hummers method: Solvent influence," Procedia Eng. **184**, 469–477 (2017).
[23]M. D. Rausch, "Metallocene chemistry—A decade of progress," Can. J. Chem. **41**, 1289–1314 (1963).
[24]R. B. Woodward, M. Rosenblum, and M. C. Whiting, "A new aromatic system," J. Am. Chem. Soc. **74**, 3458–3459 (1952).
[25]G. A. Olah, T. Yamato, T. Hashimoto, J. G. Shih, N. Trivedi, B. P. Singh, M. Piteau, and J. A. Olah, "Aromatic substitution. 53. Electrophilic nitration, halogenation, acylation, and alkylation of (.alpha.,.alpha.,.alpha.-trifluoromethoxy)benzene," J. Am. Chem. Soc. **109**, 3708–3713 (1987).
[26]D. V. Porezag and M. R. Pederson, "Optimization of Gaussian-basis sets for density functional calculations," Phys. Rev. A **60**, 2840–2847 (1999).
[27]M. R. Pederson and K. A. Jackson, "Variational mesh for quantum-mechanical simulations," Phys. Rev. B **41**, 7453–7461 (1990).
[28]J. P. Perdew, J. A. Chevary, S. H. Vosko, K. A. Jackson, M. R. Pederson, D. J. Singh, and C. Fiolhais, "Atoms, molecules, solids, and surfaces: Applications of the generalized gradient approximation for exchange and correlation," Phys. Rev. B **46**, 6671–6687 (1992).

[29]D. Porezag and M. R. Pederson, "Infrared intensities and Raman-scattering activities within density-functional theory," Phys. Rev. B **54**, 7830–7836 (1996).
[30]M. R. Pederson and S. N. Khanna, "Magnetic anisotropy barrier for spin tunneling in $Mn_{12}O_{12}$ molecules," Phys. Rev. B **60**, 9566–9572 (1999).
[31]Z. Hooshmand, J.-X. Yu, H.-P. Cheng, and M. R. Pederson, "Electronic control of strong magnetic anisotropy in Co-based single-molecule magnets," Phys. Rev. B **104**, 134411 (2021).
[32]M. R. Pederson, D. V. Porezag, J. Kortus, and D. Patton, "Strategies for massively parallel local-orbital-based electronic structure calculations," Phys. Status Solidi B **217**, 197–218 (2000).
[33]B. Paulchamy, G. Arthi, and L. Bd, "A simple approach to stepwise synthesis of graphene oxide nanomaterial," J. Nanomed. Nanotechnol. **06**, 1000253 (2015).
[34]Q. Su, S. Pang, V. Alijani, C. Li, X. Feng, and K. Müllen, "Composites of graphene with large aromatic molecules," Adv. Mater. **21**, 3191–3195 (2009).
[35]T. N. Blanton and D. Majumdar, "X-ray diffraction characterization of polymer intercalated graphite oxide," Powder Diffr. **27**, 104–107 (2012).
[36]M. B. Avinash, K. S. Subrahmanyam, Y. Sundarayya, and T. Govindaraju, "Covalent modification and exfoliation of graphene oxide using ferrocene," Nanoscale **2**, 1762–1766 (2010).
[37]J. Gao, F. Liu, Y. Liu, N. Ma, Z. Wang, and X. Zhang, "Environment-friendly method to produce graphene that employs vitamin C and amino acid," Chem. Mater. **22**, 2213–2218 (2010).
[38]K. N. Kudin, B. Ozbas, H. C. Schniepp, R. K. Prud'homme, I. A. Aksay, and R. Car, "Raman spectra of graphite oxide and functionalized graphene sheets," Nano Lett. **8**, 36–41 (2008).
[39]A. Kaniyoor and S. Ramaprabhu, "A Raman spectroscopic investigation of graphite oxide derived graphene," AIP Adv. **2**, 032183 (2012).
[40]Y. Yamada, H. Yasuda, K. Murota, M. Nakamura, T. Sodesawa, and S. Sato, "Analysis of heat-treated graphite oxide by X-ray photoelectron spectroscopy," J. Mater. Sci. **48**, 8171–8198 (2013).
[41]E. R. Lippincott and R. D. Nelson, "The vibrational spectra and structure of ferrocene and ruthenocene," Spectrochim. Acta **10**, 307–329 (1957).
[42]V. Kumar, A. Kumar, D.-J. Lee, and S.-S. Park, "Estimation of number of graphene layers using different methods: A focused review," Materials **14**, 4590 (2021).
[43]A. A. El-Gendy, E. M. M. Ibrahim, V. O. Khavrus, Y. Krupskaya, S. Hampel, A. Leonhardt, B. Büchner, and R. Klingeler, "The synthesis of carbon coated Fe, Co and Ni nanoparticles and an examination of their magnetic properties," Carbon **47**, 2821–2828 (2009).
[44]A. A. El-Gendy, M. Bertino, D. Clifford, M. Qian, S. N. Khanna, and E. E. Carpenter, "Experimental evidence for the formation of $CoFe_2C$ phase with colossal magnetocrystalline-anisotropy," Appl. Phys. Lett. **106**, 213109 (2015).
[45]R. V. Viesser, L. C. Ducati, C. F. Tormena, and J. Autschbach, "The unexpected roles of σ and π orbitals in electron donor and acceptor group effects on the ^{13}C NMR chemical shifts in substituted benzenes," Chem. Sci. **8**, 6570–6576 (2017).
[46]T. Enoki, M. Enomoto, M. Enomoto, K. Yamaguchi, N. Yoneyama, J. Yamaura, A. Miyazaki, and G. Saito, "Molecular magnets based on charge transfer complexes," Mol. Cyst. Liq. Cyst. **285**, 19–26 (1996).
[47]W. Wang, L.-Q. Yan, J.-Z. Cong, Y.-L. Zhao, F. Wang, S.-P. Shen, T. Zou, D. Zhang, S.-G. Wang, X.-F. Han, and Y. Sun, "Magnetoelectric coupling in the paramagnetic state of a metal-organic framework," Sci. Rep. **3**, 2024 (2013).